Clim Dyn (2018) 50:1335–1351
DOI 10.1007/s00382-017-3688-8

May common model biases reduce CMIP5's ability to simulate the recent Pacific La Niña-like cooling?

Jing-Jia Luo[1] · **Gang Wang**[2] · **Dietmar Dommenget**[3]

Received: 12 January 2017 / Accepted: 11 April 2017 / Published online: 18 April 2017

Abstract Over the recent three decades sea surface temperate (SST) in the eastern equatorial Pacific has decreased, which helps reduce the rate of global warming. However, most CMIP5 model simulations with historical radiative forcing do not reproduce this Pacific La Niña-like cooling. Based on the assumption of "perfect" models, previous studies have suggested that errors in simulated internal climate variations and/or external radiative forcing may cause the discrepancy between the multi-model simulations and the observation. But the exact causes remain unclear. Recent studies have suggested that observed SST warming in the other two ocean basins in past decades and the thermostat mechanism in the Pacific in response to increased radiative forcing may also play an important role in driving this La Niña-like cooling. Here, we investigate an alternative hypothesis that common biases of current state-of-the-art climate models may deteriorate the models' ability and can also contribute to this multi-model simulations-observation discrepancy. Our results suggest that underestimated inter-basin warming contrast across the three tropical oceans, overestimated surface net heat flux and underestimated local SST-cloud negative feedback in the equatorial Pacific may favor an El Niño-like warming bias in the models. Effects of the three common model biases do not cancel one another and jointly explain ~50% of the total variance of the discrepancies between the observation and individual models' ensemble mean simulations of the Pacific SST trend. Further efforts on reducing common model biases could help improve simulations of the externally forced climate trends and the multi-decadal climate fluctuations.

Keywords Pacific cooling trend · CMIP5 simulations · Common model biases · Air–sea interactions · Inter-basin influence

1 Introduction

The tropical Pacific climate, particularly the El Niño-Southern Oscillation (ENSO), has important impacts on global temperature (e.g., Pan and Oort 1983). During the recent three decades (1981–2010) sea surface temperature (SST) in the eastern equatorial Pacific has decreased (e.g., McPhaden et al. 2011; Luo et al. 2012), which may have contributed to a slowed warming of global mean surface temperature during the late 1990s–2013 (e.g., Kosaka and Xie 2013; Fyfe and Gillett 2014). The recent Pacific climate trend is robust across different observations (Fig. 1a). The cooling in the eastern Pacific and warming in the west is coupled with intensified easterlies in the western-central Pacific; this feature is reminiscent of what is observed during La Niña years. However, a key difference is that SSTs in the Indian Ocean and Atlantic have also risen rapidly in the recent decades despite the influence of the Pacific La Niña-like cooling (e.g., Klein et al. 1999). Multi-model ensemble mean of the Coupled Model Intercomparison Project Phase 5 (CMIP5) Historical simulations (Table 1), ideally representative of climate response to external radiative forcing, does not simulate this La Niña-like cooling or the associated intensification of the Walker Circulation over the same

✉ Jing-Jia Luo
j.luo@bom.gov.au

[1] Bureau of Meteorology, Level 9, 700 Collins Street, Docklands, Melbourne, VIC 3008, Australia

[2] Department of Atmospheric and Oceanic Sciences, University of Colorado Boulder, Boulder, USA

[3] School of Earth, Atmosphere and Environment, Monash University, Melbourne, Australia

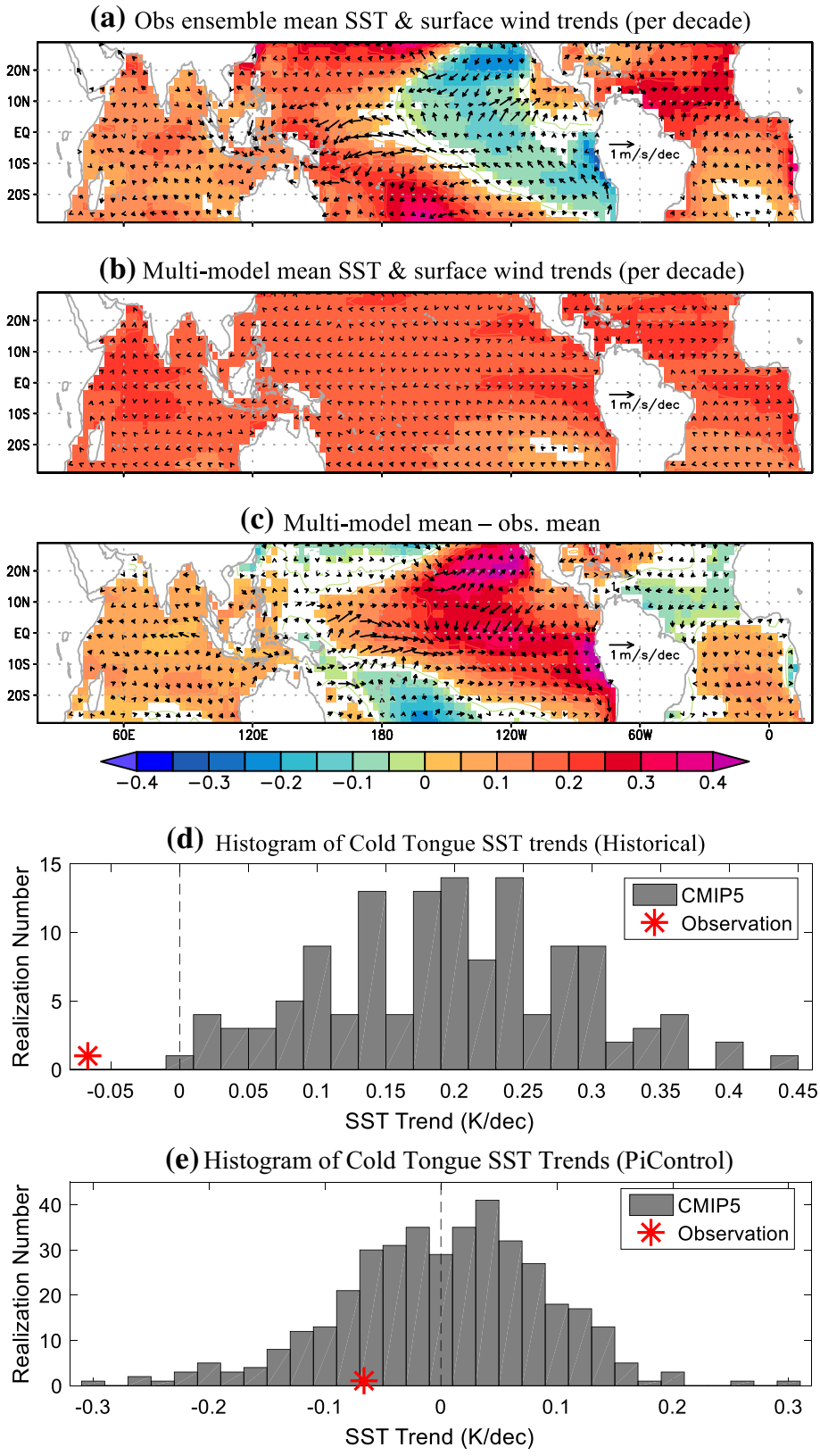

Fig. 1 Linear trends of annual mean SST and surface wind anomalies in the tropics during 1981–2010. **a** Ensemble mean of four observations (see Sect. 2). *Color shading* and *bold vectors* indicate the sign agrees among all different observational datasets. **b** Ensemble mean of 38 CMIP5 model Historical simulations (Table 1). The *color shading* and *bold vectors* indicate that at least 67% of the models produce the same sign trends as the ensemble mean. This is to assess whether the ensemble mean trends are present in a majority of the models. Note that the number of the realizations of individual models varies from 1 to 17. Model ensemble mean is used to represent individual model's results and to calculate the multi-model ensemble mean (see Sect. 2). This approach is used throughout the analysis except where explicitly stated otherwise. **c** As in **b**, but for the difference between the multi-model ensemble mean and the observational mean. **d** Histogram of the observed mean trend (*red asterisk*) and model SST trends (*grey bars*) in the cold tongue area (CT, 170°W–90°W, 5°S–5°N) based on total 126 realizations of the 38 CMIP5 model Historical simulations during 1981–2010. **e** As in **d**, but for the results based on the PiControl experiments with 392 realizations of 30-year trends

Table 1 CMIP5 models and experiments used in analysis

Number	Model name (country)	Historical	Historical Aer (ending year)	Historical Nat (ending year)	AMIP (ending year)	PiControl (100 years)
1	ACCESS1.0 (Australia)	Y			Y (2008)	Y
2	ACCESS1.3 (Australia)	Y				Y
3	BNU-ESM (China)	Y		Y (2005)	Y (2008)	Y
4	CCSM4 (USA)	Y[a]		Y (2005)	Y (2010)	Y
5	CESM1-BGC (USA)	Y[a]				Y
6	CESM1-CAM5 (USA)	Y[a]		Y (2005)	Y (2005)	Y
7	CESM1-WACCM (USA)	Y[a]				Y
8	CMCC-CM (Italy)	Y			Y (2008)	Y
9	CMCC-CMS (Italy)	Y				Y
10	CNRM-CM5 (France)	Y		Y (2010)	Y (2008)	Y
11	CSIRO-Mk3-6-0 (Australia)	Y	Y (2010)	Y (2010)	Y (2009)	Y
12	CanESM2 (Canada)	Y	Y (2010)	Y (2010)	Y (2009)	Y
13	FGOALS-g2 (China)	Y[a]	Y (2005)	Y (2009)		Y
14	GFDL-CM3 (USA)	Y	Y (2005)	Y (2005)	Y (2008)	Y
15	GFDL-ESM2G (USA)	Y			Y (2008)	Y
16	GFDL-ESM2M (USA)	Y	Y (2005)	Y (2005)	Y (2008)	Y
17	GISS-E2-H-CC (USA)	Y				Y
18	GISS-E2-H (USA)	Y	Y (2005)	Y (2010)		Y
19	GISS-E2-R-CC (USA)	Y				Y
20	GISS-E2-R (USA)	Y	Y (2005)	Y (2010)	Y (2010)	Y
21	HadCM3 (UK)	Y				
22	HadGEM2-AO (UK)	Y[b]			Y (2008)	
23	HadGEM2-CC (UK)	Y				Y
24	HadGEM2-ES (UK)	Y		Y (2010)		Y
25	IPSL-CM5A-LR (France)	Y	Y (2005)	Y (2010)	Y (2008)	Y
26	IPSL-CM5A-MR (France)	Y		Y (2010)	Y (2008)	Y
27	MIROC-ESM-CHEM (Japan)	Y		Y (2005)		Y
28	MIROC-ESM (Japan)	Y		Y (2005)		Y
29	MIROC4h (Japan)	Y				Y
30	MIROC5 (Japan)	Y			Y (2008)	Y
31	MPI-ESM-LR (Germany)	Y			Y (2009)	Y
32	MPI-ESM-MR (Germany)	Y			Y (2008)	Y
33	MRI-CGCM3 (Japan)	Y		Y (2005)	Y (2010)	Y
34	NorESM1-M (Norway)	Y	Y (2010)	Y (2010)	Y (2008)	Y
35	NorESM1-ME (Norway)	Y				Y
36	bcc-csm1-1-m (China)	Y			Y (2008)	Y
37	bcc-csm1-1 (China)	Y		Y (2010)	Y (2008)	Y
38	inmcm4 (Russia)	Y			Y (2008)	Y

These are simulations with all historical radiative forcing (Historical), historical anthropogenic aerosol forcing only (Historical Aer), and historical natural forcing only (Historical Nat) based on CMIP5 coupled models, and atmosphere stand-alone model experiments with observed SST and sea ice forcing (AMIP). All historical simulations end in 2005 while the other experiments end between 2005 and 2010. In addition, last 100-year model simulations with preindustrial radiative forcing (PiControl) are analyzed. Detailed information on each model and each experiment is available at http://pcmdi9.llnl.gov/

[a]No surface wind output

[b]No surface net flux output

period (e.g., Kociuba and Power 2015). Instead, a majority of the models produce wide SST warming across the three tropical oceans with an El Niño-like warming bias in the Pacific and slightly overestimated warming in the Indian Ocean and parts of the Atlantic (Fig. 1b, c).

With the assumption of "perfect" models, one may argue that the recent Pacific La Niña-like cooling can be generated by internal climate variability (e.g., Kosaka and Xie 2013; Watanabe et al. 2014; Risbey et al. 2014; Meehl et al. 2014), such as Pacific Decadal Oscillation (PDO) or Interdecadal Pacific Oscillation (IPO) or decadal ENSO-like variation (e.g., Mantua et al. 1997; Power et al. 1999; Zhang et al. 1997; Luo and Yamagata 2001), since the observed climate trend differs from the model ensemble mean. Based on the importance of ocean dynamics, one hypothesis (among others) is that the Pacific decadal/multi-decadal oscillation can be induced by slowly-varying subsurface signals from the subtropics (e.g., Gu and Philander 1997; Luo and Yamagata 2001). However, no persistent cold subsurface signals from either the North Pacific or the South Pacific that may induce the recent La Niña-like cooling are found in observations (e.g., Luo et al. 2012). Note that, given that the dynamics of decadal/multidecadal Pacific variability remains poorly understood (e.g., Mantua and Hare 2002), this does not deny the possible roles of other internal processes. Indeed, existing studies have suggested that the recent Pacific cooling may be induced by a combination of internal variability (e.g., IPO or PDO) and external forcing (e.g., Meehl et al. 2011, 2013; Luo et al. 2012; Marotzke and Forster 2015; Kosaka and Xie 2013; England et al. 2014; Watanabe et al. 2014; Risbey et al. 2014; Roberts et al. 2015; Takahashi and Watanabe 2016; Smith et al. 2016).

Based on the total 126 realizations of the 38 CMIP5 model Historical simulations, the results show that none of the 126 model historical realizations reproduce the intensity of the observed eastern Pacific cooling (Fig. 1d) and only one simulation produces a weak cooling (−0.007 °C per decade). Results based on a shorter period (1993–2012) are similar (e.g., Fyfe and Gillett 2014). Note that, while the global mean surface temperature has displayed a robust warming in response to the increased radiative forcing over the past century, it has been disputed whether the tropical Pacific response is an El Niño-like or La Niña-like trend (e.g., Clement et al. 1996; Seager and Murtugudde 1997; Vecchi 2008; DiNezio et al. 2009; Li et al. 2015). After removing interannual ENSO signals, Solomon and Newman (2012) have found a consistent and robust La Niña-like trend among four different reconstructed observations during 1900–2010 (see their Fig. 5), in agreement with the previous studies (e.g., Cane et al. 1997; Zhang et al. 2010). The La Niña-like cooling during the recent three decades (Fig. 1a) is similar to their robust 111-year trend. If the recent La Niña-like cooling were fully generated by internal variabilities (that is, assuming that external radiative forcing did not play any role in the generation of the Pacific cooling), the models' historical and pre-industrial simulations would display a similar ability to simulate the La Niña-like cooling. In contrast, model experiments with fixed pre-industrial radiative forcing display a good (albeit maybe not perfect) ability to produce the intensity of the observed Pacific cooling (Fig. 1e). This suggests that models' deficiencies in simulating internal variabilities (e.g., IPO or PDO) alone cannot explain the models' failure to reproduce the recent La Niña-like cooling. Besides, it is found that the multi-model mean bias in the eastern tropical Pacific is far larger than the model spread (Fig. 2a). Results based on the total 126 realizations are similar (Fig. 2b). These results suggest that the models may have a poor ability to simulate the recent climate trends in the eastern Pacific under global warming.

Errors in external radiative forcing may also affect the model simulations. It has been found that anthropogenic aerosol forcing may force a negative IPO or PDO in the 2000s, which helps slowdown the global warming in the past decade (e.g., Smith et al. 2016). It has been suggested that underestimated aerosol emissions in the 2000s may cause an overestimated global warming in the models (e.g., Fyfe and Gillett 2014; Schmidt et al. 2014). A recent model study of Takahashi and Watanabe (2016) has shown a positive contribution of the decreased natural aerosol forcing after the eruption of Mount Pinatubo in 1991 to the tropical SST warming (particularly in the western Pacific and the Atlantic) over the last two decades. Based on the CMIP5 historical anthropogenic aerosol forcing experiments (i.e., Historical Aer, Table 1), the results show that the historical anthropogenic aerosol forcing over the past three decades generates a wide cooling across the tropical oceans (Fig. 3a); this differs from the observed La Niña-like pattern (recall Fig. 1a). These results suggest that, although underestimated aerosol emissions in the models may have some positive contributions to a wide warming bias in the tropics, this aerosol forcing error cannot explain the strong El Niño-like warming bias in the eastern Pacific.

Recent studies have suggested that the observed SST warming in the tropical Atlantic and the Indian Ocean in the past decades, which may be partly forced by the increased radiative forcing (cf., Fig. 1a, b), may also play an important role in driving this La Niña-like cooling in the Pacific (e.g., Luo et al. 2012; McGregor et al. 2014; Chikamoto et al. 2015; Li et al. 2016; Takahashi and Watanabe 2016). In addition, it has been argued that, because of strong ocean dynamics in the eastern Pacific, SST in the east may rise less than that in the west in response to a uniform warming forcing (e.g., Clement et al. 1996; Cane et al. 1997; Seager and Murtugudde 1997; DiNezio et al. 2009; Zhang

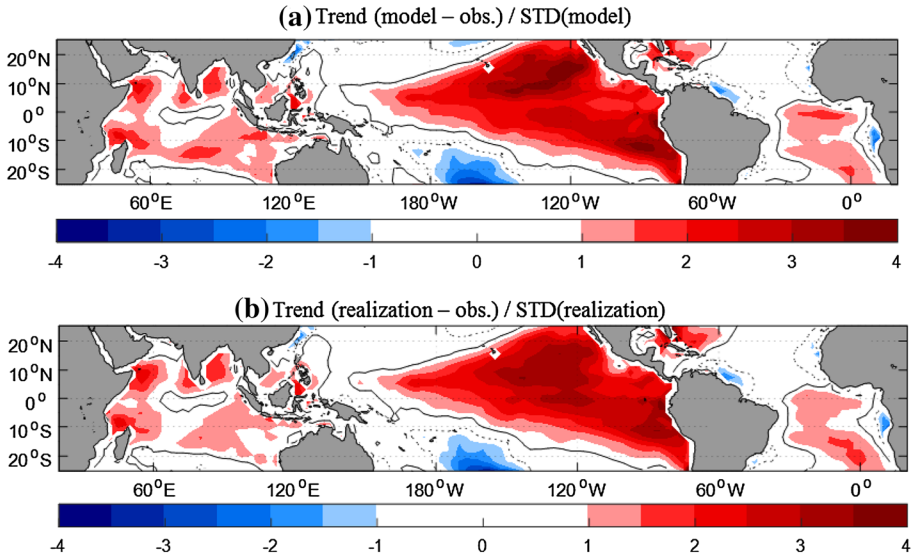

Fig. 2 Ratio between model bias and spread for the simulated SST trend during 1981–2010. **a** As in Fig. 1c, but for the ratio between the multi-model ensemble mean bias and the spread among the 38 models' ensemble mean historical simulations. The spread is calculated as one standard deviation of the SST trend differences between each model's ensemble mean and the multi-model ensemble mean. *Solid and dashed contour* indicates 0.5 and −0.5 value, respectively. **b** As in **a**, but for the ratio between the mean bias of the total 126 realizations and the spread among the 126 realizations based on the 38 CMIP5 model historical simulations

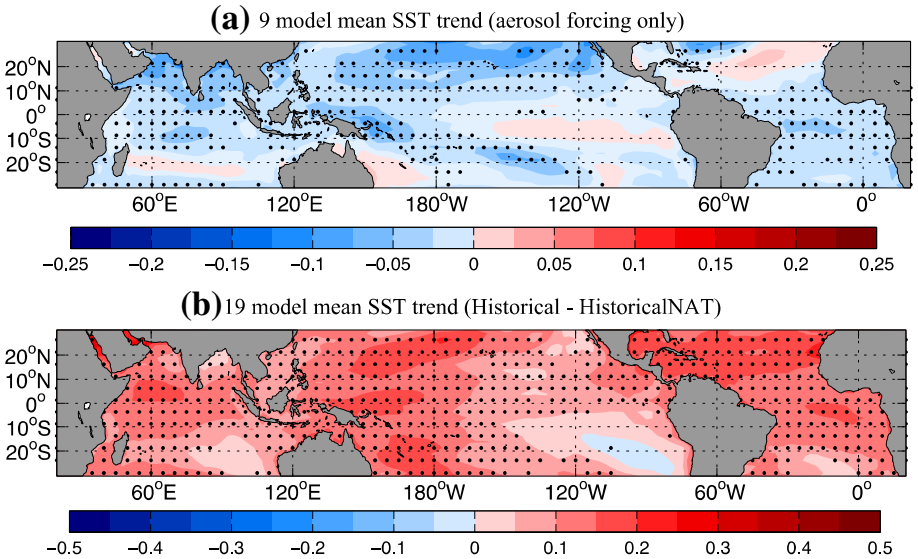

Fig. 3 Simulated multi-model ensemble mean SST trends (in °C per decade) in the tropics over the past three decades. **a** SST trends induced by historical anthropogenic aerosol forcing only. The results are based on nine CMIP5 model Historical Aer simulations (Table 1). *Stippling* indicates that at least 67% of the models produce the same sign trends as the ensemble mean. **b** As in **a**, but for the SST trends induced by anthropogenic radiative forcing only (i.e., the difference between the total historical forcing and the natural radiative forcing) based on 19 CMIP5 models (Table 1). Multi-model ensemble mean SST trends in the tropics simulated by the 19 models with total historical radiative forcing (not shown) are similar to those produced by the 38 model historical simulations (see Fig. 1b)

et al. 2010; Li et al. 2015). This ocean thermostat mechanism plus air-sea interactions in the Pacific may also contribute to a La Niña-like response to the increased greenhouse gases (GHGs) emissions. Noting that CMIP5 models display various systematic biases in simulating tropical climate (e.g., Flato et al. 2013), the "perfect model" assumption cannot be posited. It is possible that common model biases may also deteriorate the models' ability to reproduce

the internally-driven and externally-forced component of the recent Pacific La Niña-like cooling and hence contribute to the discrepancy between the multi-model simulations and the observation. But which model biases are important and how they may adversely affect the simulations of the recent Pacific climate trends are unclear.

In this study, we find several common model biases in the tropics that may favor the Pacific El Niño-like warming bias. This may contribute to the discrepancy between the multi-model simulations and the observation over the past three decades. Observations, the CMIP5 models, and methods are described in Sect. 2. Three common model biases and their possible impacts on the recent Pacific SST trend simulation are presented in Sect. 3. Summary and discussion are given in Sect. 4.

2 Methods

We use the National Oceanic and Atmospheric Administration (NOAA) extended reconstructed SST version 3b and 4 (Smith et al. 2008; Huang et al. 2015; Karl et al. 2015), NOAA Optimum Interpolation SST data (Reynolds et al. 2002), and the UK Met Office Hadley Centre's HadISST data (Rayner et al. 2003). Surface winds, surface net heat flux, total cloud cover, and pressure vertical velocity at 500 hPa level are obtained from the National Centers for Environmental Prediction (NCEP) Reanalysis 1 and 2 (Kalnay et al. 1996; Kanamitsu et al. 2002), the European Centre for Medium-Range Weather Forecasts Reanalysis (ERA-Interim) (Dee et al. 2011), and the Japanese 55-year Reanalysis (JRA-55) (Kobayashi et al. 2015). Ensemble mean of the different datasets is employed to reduce errors in the observations and to best represent the truth of the real world.

Various CMIP5 model results are used (Table 1, see also Taylor et al. 2012), including: historical simulations with total observed radiative forcing from 38 coupled models for the period 1981–2005 (Historical), sensitivity experiments from nine coupled models with only historical anthropogenic aerosol forcing (Historical Aer) and 19 coupled models with only historical natural radiative forcing (Historical Nat) for the period from 1981 to 2005, 2009 or 2010, and simulations from 23 atmosphere stand-alone models with observed SST and ice forcing (AMIP) for the period from 1981 to 2005, 2008, 2009 or 2010. We use the scenario-based projections with Representative Concentration Pathways (RCP) 4.5 to extend each model's Historical simulations from 2006 to 2010. For the AMIP, Historical Aer, and Historical Nat runs, we calculate the linear trends, climatological mean-states and correlations based on available outputs of each model. For all the four experiments, model ensemble mean calculated based on the results of individual members of each model is used to produce multi-model ensemble mean so that the weight of individual models is equal. Correlation coefficients and trends are calculated based on annual mean time series in order to reduce the influence of high-frequency signals.

In addition, CMIP5 model simulations with preindustrial radiative forcing (PiControl) are analyzed (Table 1). We select the last 100-year model outputs from individual simulations (totally 49 realizations available) and calculate the linear trends per 30 years (i.e., year 1–30, year 11–40, …, and year 71–100). The results represent internal climate variabilities simulated by the models.

It has been found that the fast SST warming in the tropical Indian Ocean and the Atlantic in the recent decades may generate an inter-basin warming contrast that contributes to the La Niña-like cooling via intensifying the Pacific trade winds (e.g., Luo et al. 2012; McGregor et al. 2014; Chikamoto et al. 2015; Li et al. 2016). The underestimated SST warming in the North Atlantic and overestimated warming in the Indian Ocean (recall Fig. 1c) and biases in reproducing the inter-basin warming contrast may impact the models' simulation of the Pacific climate trends. To examine this issue, we define the tropical (20°S–20°N) inter-basin warming contrast as the difference of the mean SST trend of the Indian Ocean (IO, 40°–120°E, with the South China Sea being excluded) and the Atlantic (Atl, 80°W–20°E) and the SST trend of the Pacific (Pac, 120°E–80°W) (see Luo et al. 2012). That is, the inter-basin warming contrast index is equal to IO/2 + Atl/2 − Pac. Possible impacts of the warming contrast between the Atlantic and the Pacific (i.e., Atl–Pac) and that between the Indian Ocean and the Pacific (i.e., IO–Pac) are also examined.

3 Model biases and impacts

In response to increased historical anthropogenic external radiative forcing, results based on 19 CMIP5 model experiments show that SSTs in the tropical Indian Ocean, Atlantic and western Pacific may rise more rapidly (Fig. 3b), possibly due to less influence from the cold subsurface there. The impacts of the historical anthropogenic external forcing are estimated with the multi-model ensemble mean differences between the Historical simulations and the simulations with historical natural radiative forcing only (i.e., Historical Nat, see Table 1). In the 38 CMIP5 model Historical simulations, the simulated SST trends during 1981–2010 in the tropical Pacific are positively correlated with those in the Atlantic and the Indian Ocean, respectively (with the two correlations being ~0.7, not shown). And most of the 38 models overestimate the SST warming in all the three tropical oceans (recall Fig. 1c). Recent studies have suggested that inter-basin warming contrasts

between the Indian Ocean/Atlantic and the Pacific, in addition to the west-east warming contrast in the Pacific itself in association with the thermostat mechanism (e.g., Clement et al. 1996; Cane et al. 1997), can modify the Walker circulation and induce easterly anomalies in the western-central Pacific, which helps generate the La Niña-like cooling via active air-sea interactions in the Pacific (e.g., Luo et al. 2012; McGregor et al. 2014; Chikamoto et al. 2015; Li et al. 2016). We find that the observed inter-basin warming contrast during 1981–2010 is rarely simulated by internal variabilities (probability = 0.25% with a skewness of −0.03, Fig. 4a). In contrast, it is better simulated with the historical radiative forcing (probability = 4%) and the distribution shows an asymmetric tail extending toward more positive values with a skewness of 0.25 (Fig. 4b). This suggests that increased external radiative forcing may have contributed to the positive inter-basin warming contrast in the recent decades (recall Fig. 3b, see also Takahashi and Watanabe 2016).

While the CMIP5 models simulate high correlations between the inter-basin warming contrasts and the SST/wind trends in the Pacific, the models underestimate the observed strengths of the inter-basin warming contrasts and the Pacific SST/easterly trends (Figs. 5, 6). Note that, with realistic SST forcing, the AMIP runs can reproduce the observed easterly trend well. The results show comparable correlation coefficients between the Indian Ocean-minus-Pacific and the Atlantic-minus-Pacific warming contrasts and the Pacific SST/wind trends (cf., Figs. 5, 6), albeit a large variety among the models' results exists. This indicates that both the tropical Indian Ocean and Atlantic SST warming may play an equivalently important role in influencing the Pacific climate trends. Note that, in the observations, the SST cooling during 1981–2010 in the cold tongue area (CT, 170°W–90°W, 5°S–5°N) is opposite to a positive Pacific (20°S–20°N, 120°E–80°W) basin-mean SST trend. In the Historical simulations, due to the model's strong El Niño-like warming bias (recall Fig. 1c), the CT SST trend may have the same sign as the Pacific basin-mean SST trend in many models. We have calculated a modified Pacific index in which the SST trends in the CT region have been excluded in the calculation of the Pacific basin-mean trend, so that the inter-basin warming contrasts between the Atlantic/Indian Ocean index and the modified Pacific index are independent to the CT SST trend. Results based on this modified Pacific index show a similar relation between the simulated CT SST trend and the modified inter-basin warming contrasts (not shown, see Fig. 5).

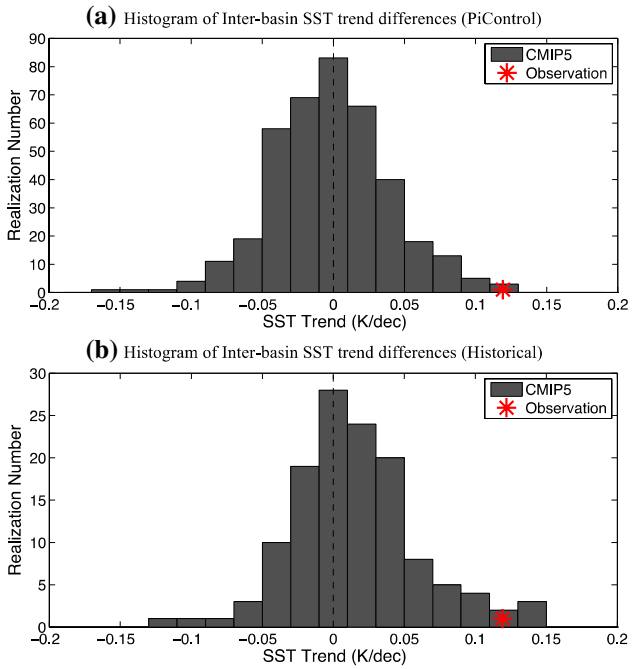

Fig. 4 CMIP5 model simulations of the inter-basin warming contrasts (i.e., IO/2 + Atl/2 − Pac). **a** Histogram of the observational mean inter-basin warming contrast between the tropical (20°S–20°N) Indian Ocean-Atlantic and the tropical Pacific during 1981–2010 (*red asterisk*) and CMIP5 PiControl experiments with 392 realizations of 30-year trends (see Sect. 2). Only one of the 392 realizations ($p = 0.25\%$) captures the intensity of the observed inter-basin warming contrast. **b** As in **a**, but for the total 126 realizations of the 38 CMIP5 model Historical simulations (1981–2010). Five of the 126 realizations ($p = 4\%$) reproduce the intensity of the observed inter-basin warming contrast

SST anomalies in the Atlantic, Indian Ocean, and Pacific can influence one another via atmospheric bridge (e.g., Klein et al. 1999) with maximum lead-lag correlations occurring at months-seasons timescale (Fig. 7). To clearly capture the inter-basin lead-lag relationships, monthly SST anomalies have been adopted. Negative (positive) lead months indicate that the CT SST anomalies lag (lead) the tropical Indian Ocean–Atlantic anomalies. The lead-lag correlations based on each member of each model have been calculated and then averaged to obtain the ensemble mean correlations of each model (see Sect. 2). Multi-model ensemble mean correlations are calculated by the average of individual model's ensemble mean. The results suggest that most models overestimate the positive influence of ENSO on the Indian Ocean–Atlantic (i.e., Atl/2 + IO/2), but the negative impact of the two oceans on the Pacific is underestimated (Fig. 7a). This model bias is more apparent in the lead-lag correlations between the CT and the Atlantic (Fig. 7b, see also Ham and Kug 2015 for the underestimated Atlantic influence on the Pacific). We find that the negative influence of the Indian Ocean on the Pacific is also underestimated, though the ENSO's positive influence on the Indian Ocean is realistically simulated (Fig. 7c, CT leads the Indian Ocean for about 5 months). We have also examined the lead-lag regressions for the three tropical oceans; results based on the regressions are similar (not

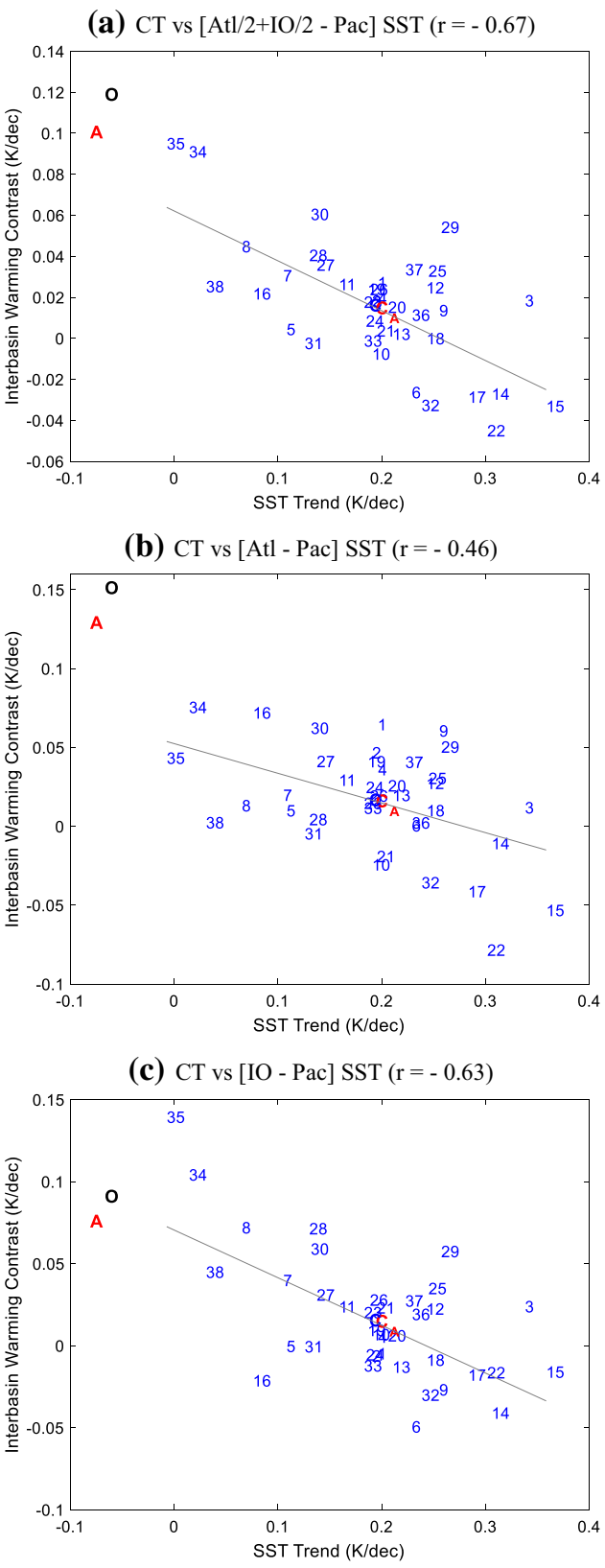

Fig. 5 CMIP5 Historical simulations of the inter-basin warming contrasts and the CT SST trends during 1981–2010. **a**–**c** Scatter plot of the CT SST trends (averaged in 170°W–90°W, 5°S–5°N) and the inter-basin warming contrasts between the tropical (20°S–20°N) Indian Ocean–Atlantic and the Pacific (i.e., Atl/2 + IO/2 − Pac), between the tropical Atlantic and the Pacific (i.e., Atl − Pac), and between the tropical Indian Ocean and the Pacific (i.e., IO − Pac). *Grey line* displays the best linear fit to the 38 model Historical simulations (i.e., ensemble mean for each model) with the correlation coefficient being indicated in panel title (magnitudes greater than 0.3 are significant at <5% level according to Student's *t* test). The ensemble mean of the observations, multi-model ensemble mean of the 38 CMIP5 model Historical simulations, the AMIP and the CMIP5 simulations with the same 23 AMIP models (Table 1) is indicated by "O", "C", "A" and "C_A", respectively

shown). Besides, results with the impact of ENSO cycle being removed and based on annual mean anomalies show the similar model bias. This implies that the contribution of the Indian Ocean/Atlantic warming to the recent Pacific La Niña-like cooling may be underestimated in most models.

Although none of the 38 models reproduce the observed La Niña-like cooling, about half of the models are able to reproduce an easterly trend (albeit weak) in the western-central Pacific (150°E–150°W, 10°S–10°N) (Fig. 8a, see also England et al. 2014). Among them, 12 models better reproduce the intensified easterlies with a better simulated west-east warming gradient in the Pacific, corresponding to the stronger SST warming in the Indian Ocean and Atlantic than that in the Pacific (Fig. 9a). The inter-basin warming contrasts are better simulated. In the second group of 14 models that produce a neutral easterly trend, no clear inter-basin warming contrast is reproduced and the eastern equatorial Pacific SST warming is slightly stronger than that in the west (Fig. 9b). In contrast, in models that simulate an unrealistic El Niño-like warming with a westerly trend in the western-central Pacific, the simulated inter-basin warming contrasts are largely negative (Fig. 9c). These results suggest that errors in the simulated Pacific climate trends are linked with errors in the simulated inter-basin warming contrasts.

Besides, errors in simulating the Pacific thermostat mechanism may also contribute to the models' error in simulating the Pacific climate trends. This suggests that the models also need to correctly simulate local processes in the Pacific. A majority of the models produce an unrealistic El Niño-like east–west SST trend gradient in the Pacific with a correlation of 0.45 between the east–west SST trend gradient and the CT SST trend (Fig. 8b). The east–west gradient is calculated with the SST trend difference between the western (10°S–10°N, 120°E–180°) and eastern Pacific (10°S–10°N, 180°–80°W). About 10 out of the 38 models reproduce a negative east–west SST trend gradient but only one model captures the intensity of the observed La Niña-like trend gradient in the Pacific. The underestimated

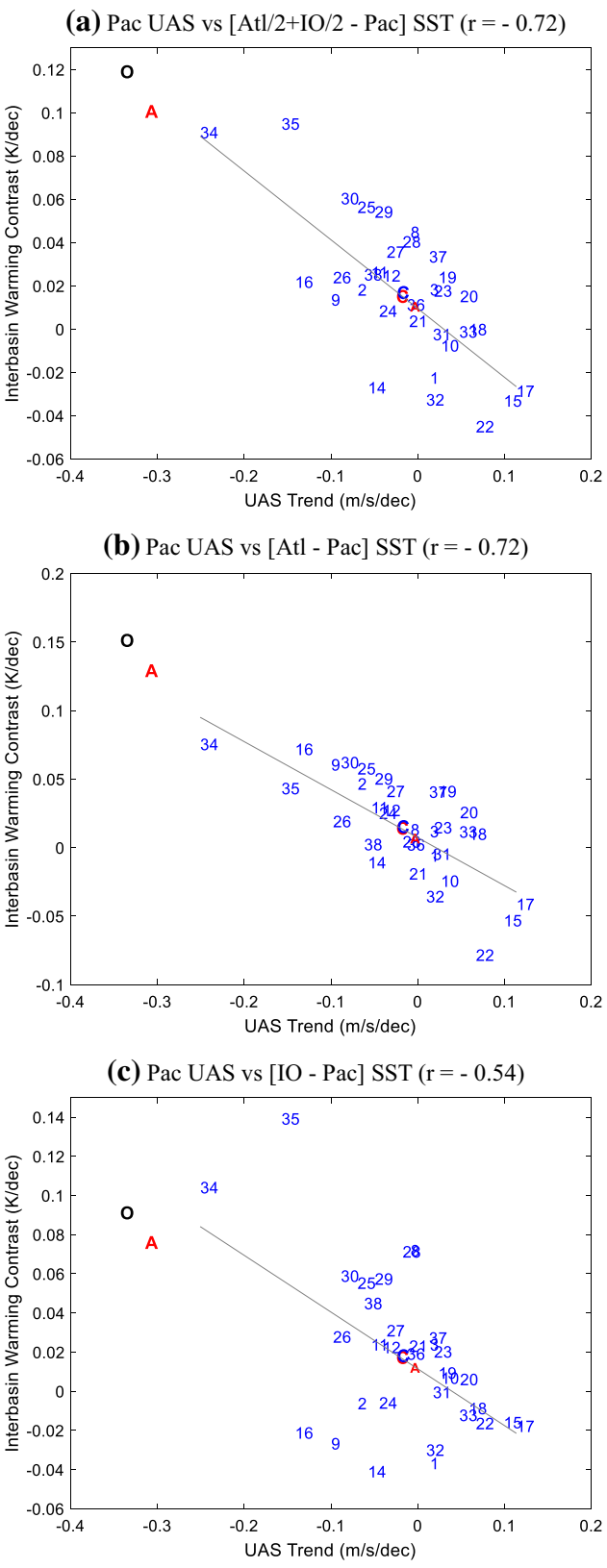

Fig. 6 CMIP5 Historical simulations of the inter-basin SST warming contrasts and the easterly trends in the western-central Pacific during 1981–2010. **a**–**c** As in Fig. 5, but for results based on the simulated easterly trends in the western-central Pacific (150°E–150°W, 10°S–10°N). *Grey lines* display the best linear fit to 33 CMIP5 model historical simulations (Table 1). The ensemble mean of the observations, multi-model ensemble mean of the 33 CMIP5 model historical simulations, the AMIP and CMIP5 simulations with the same 18 AMIP models is indicated by "O", "C", "A" and "C_A", respectively

easterly trends in the western-central Pacific are also correlated with the poorly simulated east–west SST trend gradients with a correlation of 0.6 (Fig. 8c). In addition, while the models simulate a high correlation between the SST and the wind trends in the Pacific, the easterly trends do not induce a cooling in the east (recall Fig. 8a). This is consistent with previous findings that the ocean response to wind forcing and the wind-thermocline-SST feedback associated with ENSO are underestimated (e.g., Bellenger et al. 2014; Kim et al. 2014), partly associated with too diffusive equatorial thermocline (e.g., Flato et al. 2013). The results suggest that the Pacific thermostat mechanism may also be underestimated in the models.

Another long-standing coupled model bias in the tropical Pacific is that the simulated cold tongue extends too far to the west, leading to a cold SST mean-state bias across the equatorial basin (Figs. 10a, 11a) (e.g., Flato et al. 2013; Luo et al. 2005), except the region near the west coast of South America where most models display a strong warm bias owing to underestimated stratus clouds and poorly resolved ocean eddies and coastal upwelling (e.g., Flato et al. 2013). The cold SST mean-state bias acts to reduce atmospheric deep convection (allowing more solar insolation to reach the sea surface) and decrease surface evaporation (i.e., less heat loss from the ocean) (figures not shown). This leads to an overestimated net heat flux into ocean in the equatorial Pacific (120°E–90°W, 5°S–5°N) (Figs. 10b, 11b), which can positively contribute to the Pacific SST warming bias according to the mixed layer heat budget equation: $dT'/dt = Q'/(\rho\ c\ H) + F'_{ocean}$, where dT'/dt is the SST tendency bias, Q' and F'_{ocean} refers to the bias in the surface net heat flux and total ocean processes, respectively, ρ, c, and H is the density and specific heat of water, and mixed layer depth, respectively. Integrating this simple equation for the period 1981–2010 gives that the bias in the SST trend over the past three decades is determined by the net bias of the 30-year mean $Q'/(\rho\ c\ H)$ (i.e., heat flux forcing) and F'_{ocean}.

Note that, by comparing to the atmospheric reanalysis heat fluxes rather than other products estimated with in situ observations, impacts of some systematic biases in both the reanalysis models and CMIP5 models (such as underestimated stratus clouds in the eastern Pacific) can be partly removed. The positive 30-year mean Q' can be

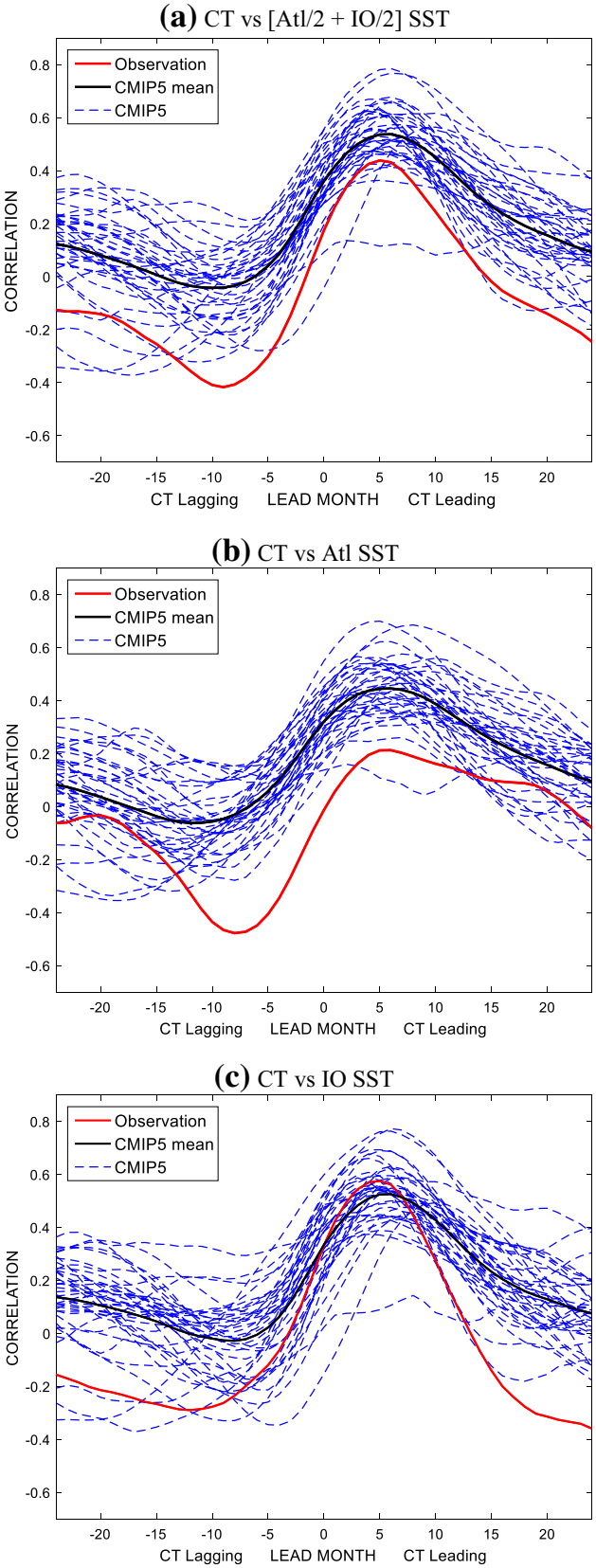

Fig. 7 CMIP5 historical simulations of the inter-basin influences during 1981–2010. **a–c** Lead-lag correlations of monthly SST anomalies between the Pacific CT area and the tropical (20°S–20°N) Atlantic–Indian Ocean (i.e., Atl/2 + IO/2), between the CT and the tropical Atlantic, and between the CT and the Indian Ocean. The *red* (*black*) *solid line* denotes the observed (multi-model ensemble mean) lead-lag correlations. The *blue dashed-lines* denote the ensemble mean correlations for each model. Results based on different latitudinal bands (e.g., 10°S–10°N or 5°S–5°N) in the Indian Ocean and Atlantic are similar

a consequence of some combination of biases in simulating atmosphere–ocean equilibrium state with fixed external forcing and biases in simulating response to increased external forcing and/or internal decadal/multidecadal variability. And it is generally possible that the 30-year mean F'_{ocean} may largely offset or even over-compensate the positive bias of the heat flux forcing. Only a very small fraction of the positive 30-year mean Q′ (less than about 0.26 or 0.52 W/m^2 if assuming H = 50 m or 100 m) is needed to explain the positive Pacific SST trend bias, but all the models produce a much large positive heat flux bias (Fig. 10b). This suggests that the F'_{ocean} in the models should be largely negative with a value being close to $-Q'/(\rho\ c\ H)$ according to the mixed layer heat budget (since dT′/dt is relatively very small). Besides, the result shows that the simulated SST trend bias in the coupled models is in positive proportion to the heat flux bias (Fig. 10b, albeit with a weak correlation of 0.34). This gives some support that a stronger positive heat flux bias in the equatorial Pacific indeed tends to induce a stronger SST warming bias in some models. With observed SST forcing, the atmosphere stand-alone models (Table 1) produce ~50% less heat flux bias in the equatorial Pacific (Figs. 10b, 11c). And the heat flux bias shows a negative correlation (−0.3) with the mean SST bias in the equatorial Pacific (Fig. 11d). The results suggest the cold SST mean-state bias may be one of important contributors to the overestimated surface net heat flux.

A related important process observed is a strong local feedback between SST and atmosphere deep convection (measured by pressure vertical velocity at the 500 hPa level) or between SST and total cloud in the equatorial Pacific except the coastal area of South America (Fig. 12a, c). Warmer SSTs induce stronger convection and hence greater cloud cover which in turn acts to dampen the warmer SSTs by reducing surface solar insolation, and vice versa (e.g., Bellenger et al. 2014; Dommenget et al. 2014). The SST-convection-cloud correlations are underestimated by most models particularly in the eastern equatorial Pacific (Fig. 12b, d). The similar bias was also found in centennial runs of CMIP5 models (e.g., Bellenger et al. 2014). The result suggests that the SST warming in the eastern Pacific could not be sufficiently dampened in the models due to the underestimated clouds; this may also

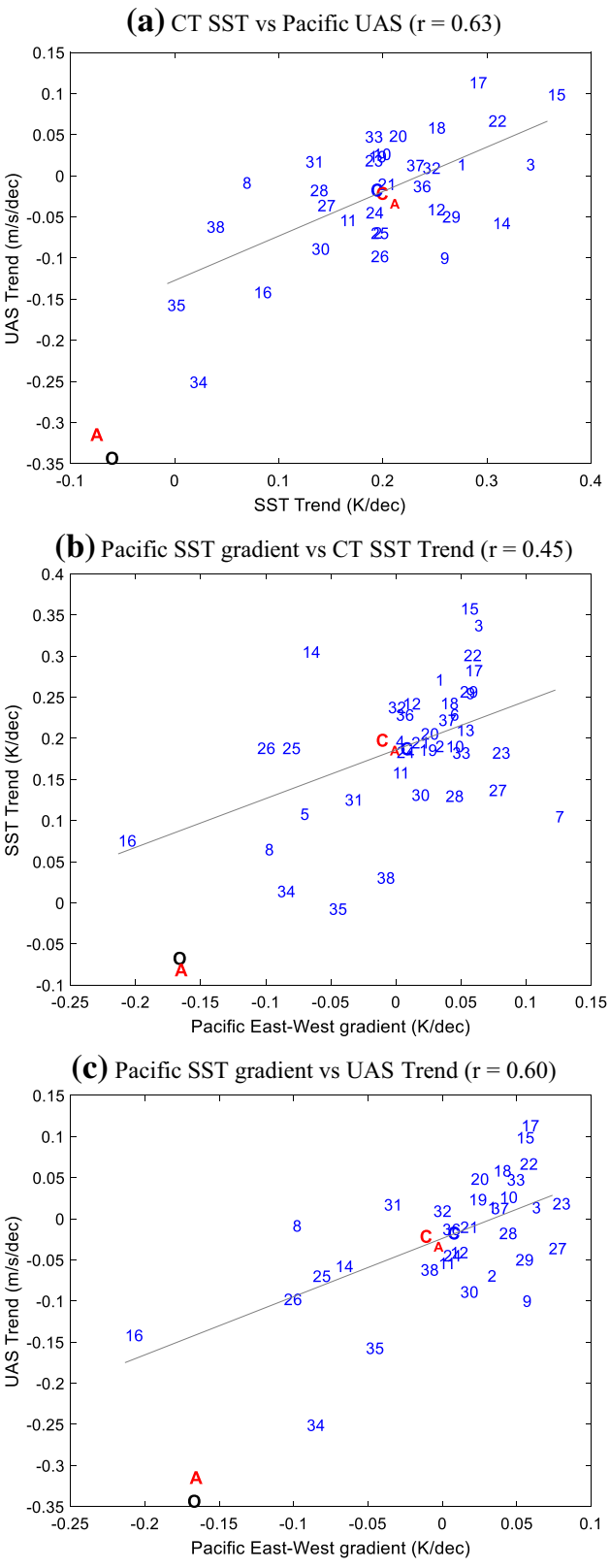

Fig. 8 **a** As in Fig. 5a, but for the scatter plot of the CT SST trends ▸ and the easterly trends in the western-central Pacific (150°E–150°W, 10°S–10°N). **b–c** As in **a**, but for the relation between the east–west SST trend gradient and the CT SST trend, and between the east–west SST trend gradient and the western-central Pacific wind trend. The east–west gradient is calculated with the SST trend difference between the western (10°S–10°N, 120°E–180°) and eastern Pacific (10°S–10°N, 180°–80°W). Results based on different eastern and western Pacific boxes with the longitude of their boundary being shifted westward or eastward for 10°–30° are similar

contribute to the El Niño-like warming bias over the past three decades (see also Guilyardi et al. 2009 for a similar discussion on ENSO simulations). Further analysis shows that the atmospheric models with observed SST forcing realistically reproduce the observed SST-cloud feedback in the eastern Pacific (Fig. 12e). However, the correlation between the simulated SST-cloud feedback and the SST mean-state in the coupled models is modest (0.38), indicating that model biases in other air–sea coupled processes may also play a role. Note that along the west coast of South America where cold SSTs increase atmospheric stability of the planetary boundary layer that favors stratus cloud formation, a positive SST-cloud feedback exists (i.e., cold SSTs induce more clouds and less surface insolation, leading to colder SSTs. See also Philander et al. 1996). The CMIP5 Historical runs also show a poor skill in simulating this feedback (Fig. 12d) partly due to the local warm SST mean-state bias; this limits the models' ability to simulate the coastal cooling.

Note that, because of the important influence of internal variability on the recent Pacific trends (e.g., Kosaka and Xie 2013; Watanabe et al. 2014; Risbey et al. 2014; Meehl et al. 2014), the model's ensemble mean may diminish the internally-induced signal, particularly for the models that have a large number of members. To address this concern, we have also examined the results based on 38 realizations (i.e., only the first member of each model's historical simulations is selected). The results are similar (see Fig. 13). Besides, results based on the total 126 realizations of the 38 models' historical simulations are also similar (not shown). This suggests that the identified model biases are robust across the three different approaches.

We have estimated the relative contributions of the three common model biases to the errors in the simulated CT SST trend by means of a multiple linear regression. That is, errors in the overestimated CT SST trend = a × [errors in the underestimated interbasin (i.e., Atl/2 + IO/2 − Pac) SST trend difference] + b × (errors in the overestimated CT heat flux) + c × (errors in the underestimated CT cloud-SST feedback). Here, the errors are defined as the discrepancies between the observation and individual models' ensemble mean simulations. It is worth noting that the defined errors contain the contributions of both the external forcing and internal climate variabilities. All the errors have been normalized before performing the multiple regressions. This gives multiple correlations: a = −0.67, b = 0.27, and

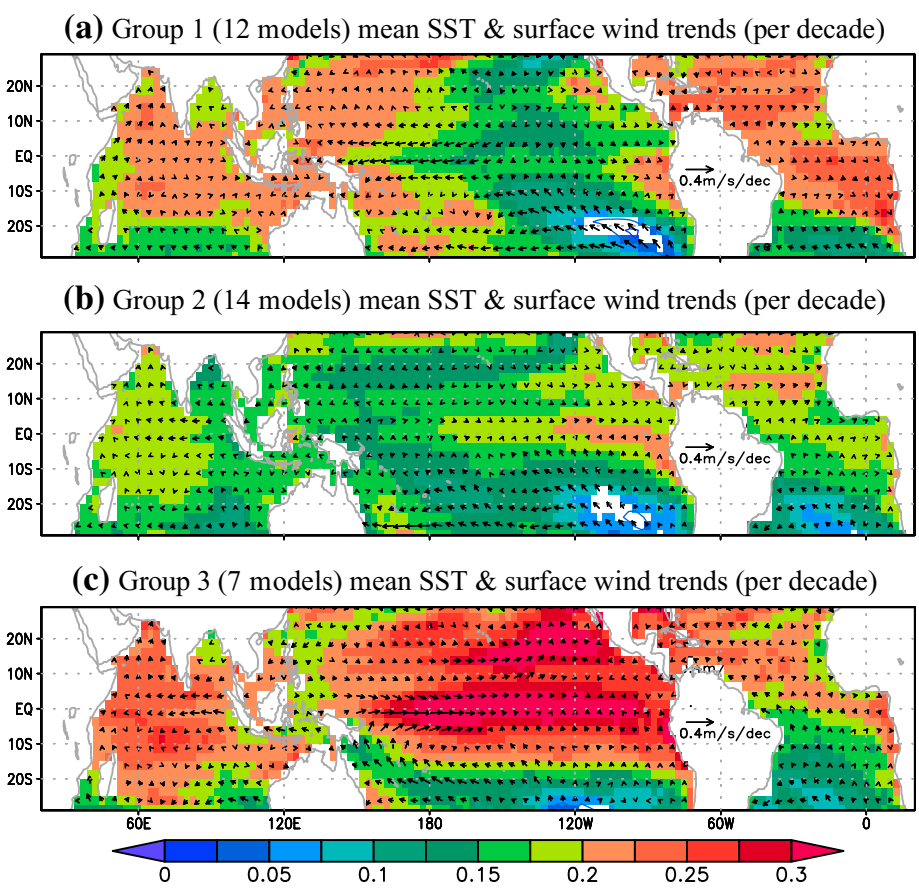

Fig. 9 Simulated multi-model ensemble mean SST and surface wind trends during 1981–2010 in three subgroups of 33 CMIP5 model historical simulations. The three subgroups are constructed with the zonal wind trends (unit: m s^{-1} per decade) in the western-central Pacific (150°E–150°W, 10°S–10°N) being <−0.05 (group 1), from −0.05 to 0.05 (group 2), and >0.05 (group 3), respectively. The *colour shading* and *bold vectors* indicate that >67% of the models in each subgroup produce the same sign trends

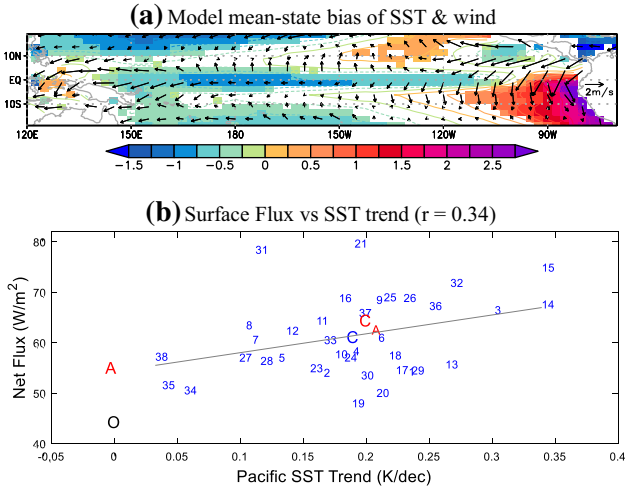

Fig. 10 CMIP5 Historical simulations of the climatological mean SST, surface winds and surface net heat flux in the equatorial Pacific during 1981–2010. **a** Differences of the climatological mean SST and surface winds between the multi-model ensemble mean and the observational mean. *Color shading* and *bold vectors* indicate that at least 67% of the models produced the same sign errors as the ensemble mean. **b** As in Fig. 5a, but for the *scatter plot* of the SST trends and the surface net heat fluxes (downward positive) in the equatorial Pacific (120°E–90°W, 5°S–5°N) based on 37 CMIP5 model Historical simulations (Table 1). Results for the CT area are similar

c = −0.17. Among the three model biases, errors in the interbasin warming contrast have a predominant contribution. Besides, the result suggests that effects of the three common model biases do not cancel one another; all of them positively contribute to the errors in the overestimated CT SST trend. The correlation between the reconstructed CT SST trend errors and the original errors is 0.7. Results based on non-normalized errors are the same. This means that nearly 50% of the total variance of the CMIP5 model errors can be explained by the three common model biases. Results based on the 38 realizations (i.e., one member per model) and the total 126 realizations are similar; the correlation between their reconstructed CT SST trend errors and the original errors is 0.78 and 0.68, respectively.

4 Summary and discussion

In summary, our results suggest that common biases of current state-of-the-art models may favor a stronger-than-observed warming in the tropical eastern Pacific (i.e., an El Niño-like warming bias) and hence may decrease the models' ability to reproduce the La Niña-like cooling over the past three decades. The inter-basin warming contrasts between the tropical Atlantic/Indian Ocean and the Pacific

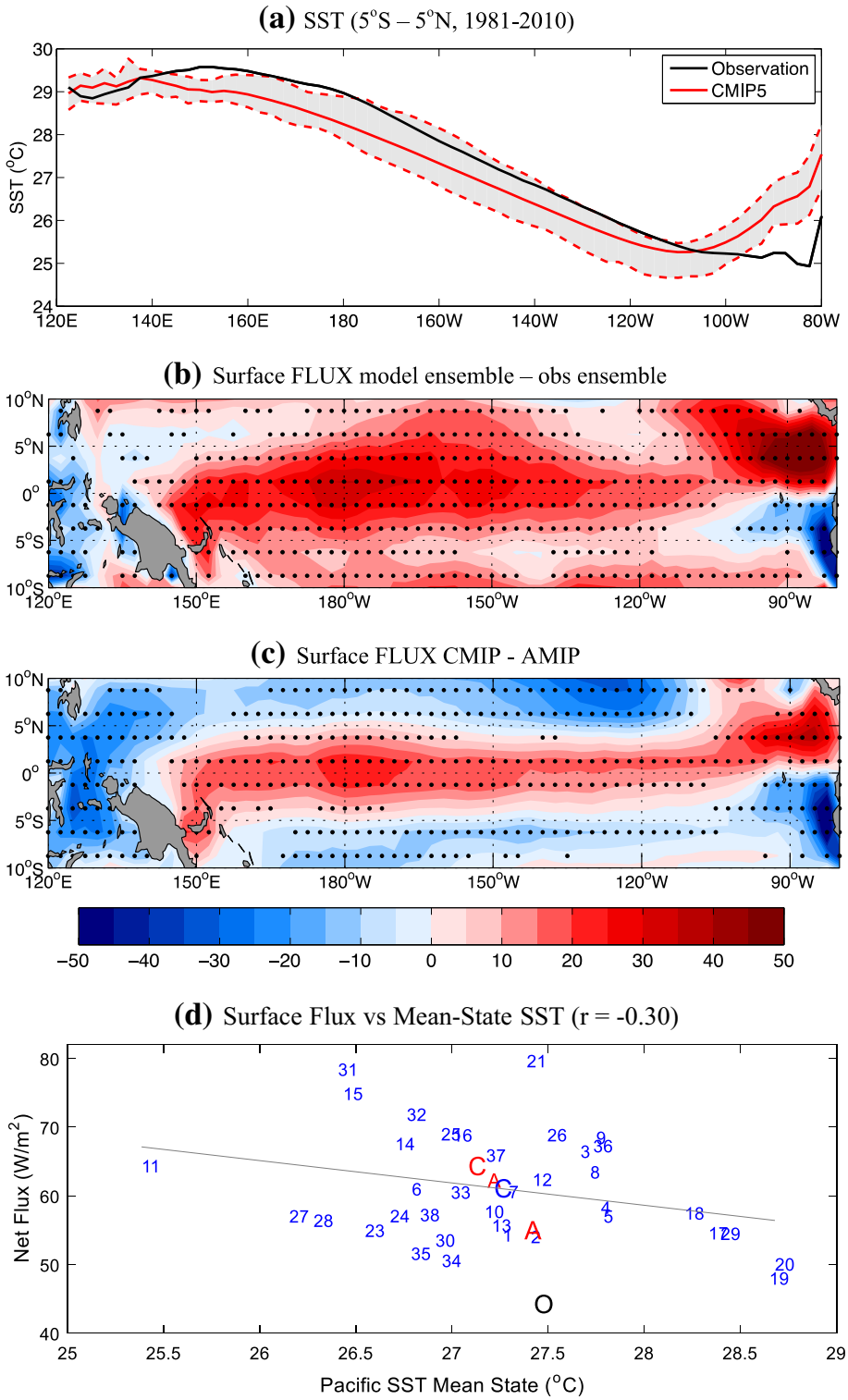

Fig. 11 CMIP5 historical simulations of the climatological mean SST and surface net heat flux in the equatorial Pacific during 1981–2010. **a** Annual mean SST climatology along the equator (5°S–5°N) based on the observational mean (*black line*) and the multi-model ensemble mean of 38 CMIP5 model Historical simulations (*red solid line*). *Grey shaded* area denotes 25–75 percentiles of the 38 model historical simulations. **b** Surface net heat flux (W m^{-2}, *downward* positive) differences between the multi-model ensemble mean of 37 CMIP5 model historical simulations (Table 1) and the observational mean. *Stippling* indicates that at least 67% of the 37 models produce the same sign errors as the ensemble mean. **c** As in **b**, but for the heat flux differences between the CMIP5 historical and the AMIP simulations based on the multi-model ensemble mean of the same 22 models (Table 1). With the models' errors being cancelled out, these differences may display more accurate impacts of the cold SST mean-state bias. **d** As in Fig. 10b, but for results based on the surface heat flux and SST mean state in the equatorial Pacific

are underestimated in most models probably owing to the underestimation of the inter-basin influences and the local wind-thermocline-SST feedback in the Pacific. Besides, possibly partly due to the cold SST mean-state bias in the equatorial Pacific, surface net heat flux is overestimated (i.e., ocean surface layer could be heated too much) but the local SST-cloud negative feedback is underestimated (i.e., the induced SST warming could not be sufficiently dampened). These models' biases in simulating the local air-sea interactions in the Pacific suggest that the Pacific thermostat mechanism may also be underestimated. These model biases may act together to produce the El Niño-like

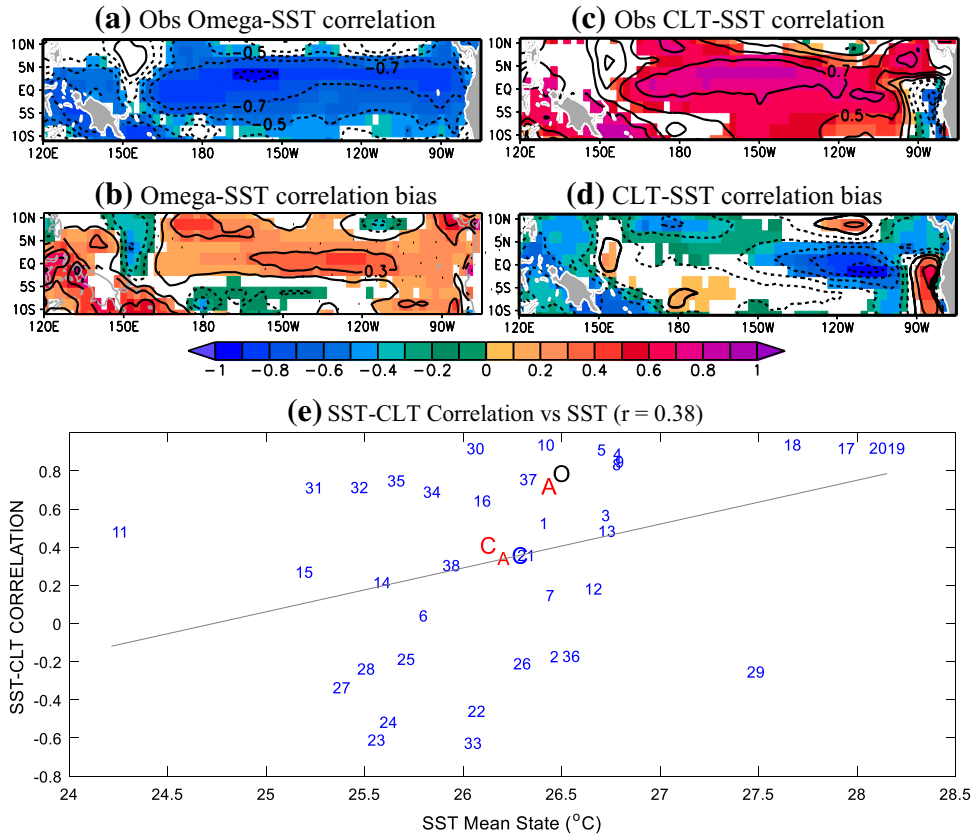

Fig. 12 CMIP5 historical simulations of the local SST-convection-cloud correlations in the equatorial Pacific during 1981–2010. **a** Correlations between the annual mean SST anomalies and pressure vertical velocity anomalies at 500 hPa level (ω in Pa s^{-1}, a negative ω means rising motion) based on the observational mean data (*contour*). Correlation coefficients above 0.3 are significant at 5% level according to Student *t* test and color shading indicates at least three of four observational datasets produce the same sign. **b** As in **a**, but for the difference between the CMIP5 multi-model ensemble mean and the observed. *Color shading* denotes at least 67% of the models produce the same sign errors as the ensemble mean. **c**–**d** As in **a**–**b**, but for the correlations between the annual mean SST and total cloud anomalies. **e** As in Fig. 10b, but for the *scatter plot* of the SST mean-states and the local SST-cloud correlations in the CT area based on the 38 CMIP5 model historical simulations. Note that results based on regressions of the local SST on convection/cloud and those based on 3-year running mean anomalies are similar

warming bias in the Pacific. Our results provide an alternative explanation to the prevailing view that errors in simulated internal climate variations and/or external radiative forcing may play a key role in causing the discrepancy between the multi-model simulations and the observation. The results contribute to address one of the CMIP6 broad questions: "what are the origins and consequences of systematic model biases?".

Note that the common model biases defined in this study contain biases in simulating both the response to external forcing and internal decadal/multi-decadal variability, although the preindustrial simulations show a good ability to produce the intensity of the recent La Niña-like cooling (recall Fig. 1e). Exact contributions of the internal variability and external forcing are unclear and need to be explored in future studies. For instance, the positive 30-year mean heat flux bias and the related cold SST mean-state bias in the equatorial Pacific could help induce an overestimated warming in the model simulations due to a relation (as described below) between CO_2 radiative forcing, cloud and water vapour in the atmosphere. The CO_2 radiative forcing is a function of the cloud and amount of water vapour in the atmosphere (e.g., Kiehl and Ramanathan 1982; Schmidt et al. 2010). The larger surface net heat flux in the model simulations could be related to less cloud and a drier atmosphere in association with the cold SST mean-state bias. A drier and less cloudy atmosphere sees a stronger thermal radiative forcing from CO_2 increase and could therefore respond more strongly to the same CO_2 increase than a more cloudy and moist atmosphere does (e.g., Dommenget and Floeter 2011). This effect may contribute to a warming bias in models, as the models have in average a bias towards a less cloudy and drier atmosphere in the equatorial Pacific. Further studies are warranted to examine how biases in the atmosphere and ocean processes act together to produce the SST trend bias in the models.

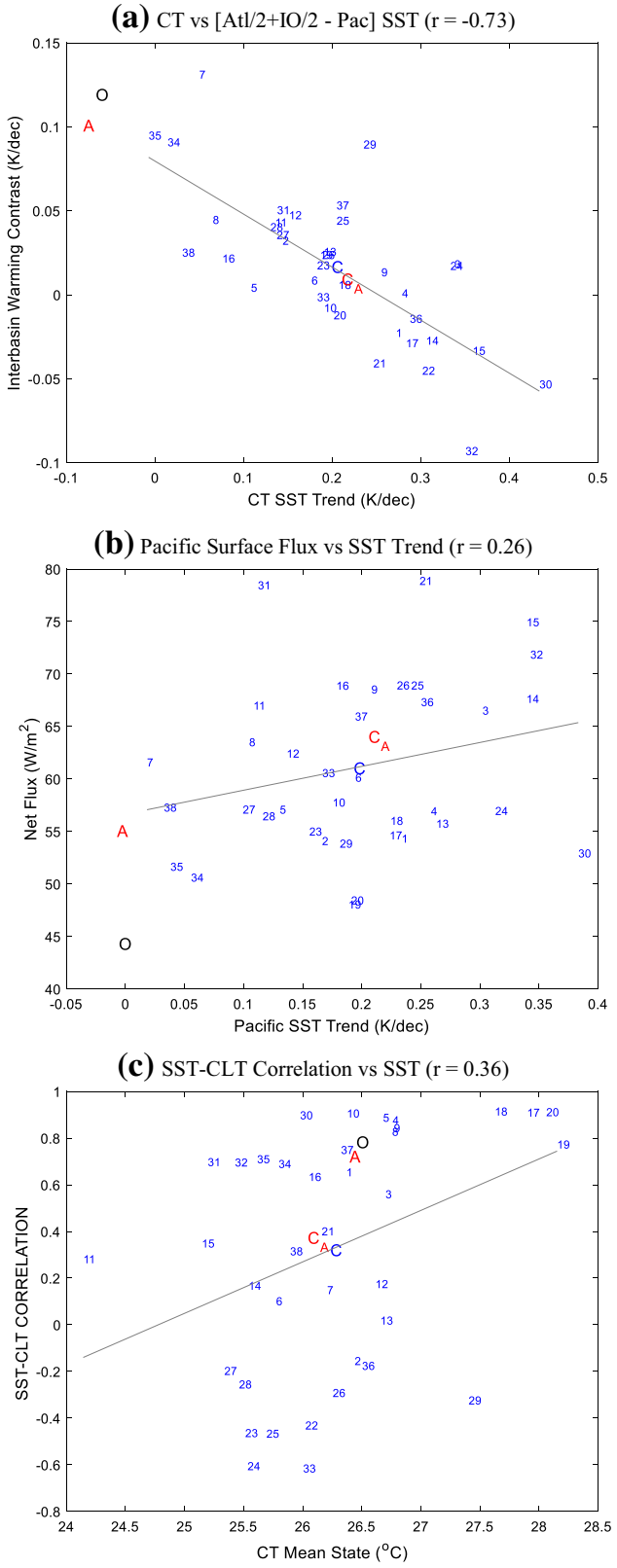

Fig. 13 As in Figs. 5a, 10b and 12e, but for results based on 38 realizations (i.e., only the first member of each model's historical simulations during 1981–2010 is selected)

It is also worth noting that other common biases in simulating ocean and atmospheric processes and their interactions may also reduce the models' ability in simulating the recent Pacific climate trends. For instance, while observations have shown frequent occurrence of central-Pacific (or Modoki) type of El Niño in recent decades (e.g., Ashok et al. 2007; McPhaden et al. 2011; Luo et al. 2012) that may affect the mean-state changes, most models favor a single type of El Niño with the eastern Pacific SST anomalies being extended too far to the west (e.g., Kug et al. 2012; Luo et al. 2005). Another possible contributor to the models' inability is that internal multi-decadal variability of the Pacific Walker Circulation may be underestimated by the models (e.g., Kociuba and Power 2015). Besides, regarding the importance of the inter-basin interactions in influencing the Pacific climate, models' errors in simulating SSTs and ocean–atmosphere processes in the Indian Ocean and the Atlantic may also deteriorate the models' ability. For instance, while multi-model ensemble mean reproduces reasonably well the SST warming trends in the Atlantic and the Indian Ocean in the recent decades, the simulated SST mean-states there are cooler than the observed (not shown). Decadal hindcasts started from realistic initial conditions can improve the simulation of the Pacific La Niña-like cooling (e.g., Meehl et al. 2014), in association with increased ocean heat up-take and the inter-basin influences (e.g., Guemas et al. 2013; Chikamoto et al. 2015). With realistic ocean conditions and hence correct long memory, common model biases can be reduced; this could improve the models' performance. Further efforts on reducing the common model biases in both the Pacific and the other two ocean basins could help improve climate predictions/projections in response to external forcing and simulations of the multi-decadal climate fluctuations.

Acknowledgements The authors thank M. Wheeler, J. Arblaster, H. Hendon, and S. McGregor for their helpful internal reviews and two anonymous reviewers for their helpful comments. G.W. and D. D. are supported by the ARC project "Beyond the linear dynamics of the El Nino Southern Oscillation" (DP120101442) and the ARC Centre of Excellence in Climate System Science (CE110001028).

References

Ashok K, Behera SK, Rao SA, Weng H, Yamagata T (2007) El Niño Modoki and its possible teleconnection. J Geophys Res 112:C11007. doi:10.1029/2006JC003798

Bellenger H, Guilyardi E, Leloup J, Lengaigne M, Vialard J (2014) ENSO representation in climate models: from CMIP3 to CMIP5. Clim Dyn 42:1999–2018

Cane MA, Clement AC, Kaplan A, Kushnir Y, Pozdnyakov D, Seager R, Zebiak SE, Murtugudde R (1997) Twentieth-century sea surface temperature trends. Science 275:957–960. doi:10.1126/science.275.5302.957

Chikamoto Y, Timmermann A, Luo JJ, Mochizuki T, Kimoto M, Watanabe M, Ishii M, Xie SP, Jin FF (2015) Skilful multi-year predictions of tropical trans-basin climate variability. Nat Commun 6:6869. doi:10.1038/ncomms7869

Clement AC, Seager R, Cane MA, Zebiak SE (1996) An ocean dynamical thermostat. J Clim 9:2190–2196

Dee DP, Uppala SM, Simmons AJ, Berrisford P, Poli P, Kobayashi S, Andrae U, Balmaseda MA, Balsamo G, Bauer P, Bechtold P, Beljaars ACM, van de Berg L, Bidlot J, Bormann N, Delsol C, Dragani R, Fuentes M, Geer AJ, Haimberger L, Healy SB, Hersbach H, Hólm EV, Isaksen L, Kållberg P, Köhler M, Matricardi M, McNally AP, Monge-Sanz BM, Morcrette JJ, Park BK, Peubey C, de Rosnay P, Tavolato C, Thépaut JN, Vitart F (2011) The ERA-Interim reanalysis: configuration and performance of the data assimilation system. Q J R Meteorol Soc 137:553–597. doi:10.1002/qj.828

DiNezio PN, Clement AC, Vecchi GA, Soden BJ, Kirtman BP (2009) Climate response of the equatorial Pacific to global warming. J Clim 22(18):4873–4892

Dommenget D, Floeter J (2011) Conceptual understanding of climate change with a globally resolved energy balance model. Clim Dyn 37:2143–2165

Dommenget D, Haase S, Bayr T, Frauen C (2014) Analysis of the slab-ocean El Niño atmospheric feedbacks in observed and simulated ENSO dynamics. Clim Dyn 42:3187–3205

England MH, McGregor S, Spence P, Meehl GA, Timmermann, A, Cai W, Sen Gupta A, McPhaden MJ, Purich A, Santoso A (2014) Recent intensification of wind-driven circulation in the Pacific and the ongoing warming hiatus. Nat Clim Change 4:222–227

Flato G, Marotzke J, Abiodun B, Braconnot P, Chou SC, Collins W, Cox P, Driouech F, Emori S, Eyring V, Forest C, Gleckler P, Guilyardi E, Jakob C, Kattsov V, Reason C, Rummukainen M (2013) Evaluation of climate models. In: Stocker TF et al (eds) Climate change 2013: the physical science basis. contribution of working group I to the fifth assessment report of the intergovernmental panel on climate change. Cambridge University Press, Cambridge, pp 741–866

Fyfe JC, Gillett NP (2014) Recent observed and simulated warming. Nat Clim Change 4:150–151

Gu DF, Philander SH (1997) Interdecadal climate fluctuations that depend on exchanges between the tropics and extratropics. Science 275:805–807

Guemas V, Doblas-Reyes FJ, Andreu-Burillo I, Asif M (2013) Retrospective prediction of the global warming slowdown in the past decade. Nat Clim Change 3:649–653

Guilyardi E, Braconnot P, Jin FF, Kim ST, Kolasinski M, Li T, Musat I (2009) Atmosphere feedbacks during ENSO in a coupled GCM with a modified atmospheric convection scheme. J Clim 22:5698–5718

Ham YG, Kug JS (2015) Role of north tropical Atlantic SST on the ENSO simulated using CMIP3 and CMIP5 models. Clim Dyn 45(11):3103–3117

Huang B, Banzon VF, Freeman E, Laurimore J, Liu W, Peterson TC, Smith TM, Thorne PW, Woodruff SD, Zhang HM (2015) Extended reconstructed sea surface temperature version 4 (ERSST.v4), Part I. upgrades and intercomparisons. J Clim 28:911–930

Kalnay E, Kanamitsu M, Kistler R, Collins W, Deaven D, Gandin L, Iredell M, Saha S, White G, Woollen J, Zhu Y, Leetmaa A, Reynolds R, Chelliah M, Ebisuzaki W, Higgins W, Janowiak J, Mo K, Ropelewski C, Wang J, Jenne R, Joseph D (1996) The NCEP/NCAR 40-year reanalysis project. Bull Am Meteor Soc 77:437–471

Kanamitsu M, Ebisuzaki W, Woollen J, Yang S, Hnilo J, Fiorino M, Potter G (2002) NCEP-DOE AMIP-II reanalysis (R-2). Bull Amer Meteor Soc 83:1631–1643

Karl TR, Arguez A, Huang B, Lawrimore JH, McMahon JR, Menne MJ, Peterson TC, Vose RS, Zhang HM (2015) Possible artifacts of data biases in the recent surface warming hiatus. Science 348:1066–1067

Kiehl JT, Ramanathan V (1982) Radiative heating due to increased CO_2—the role of H_2O continuum absorption in the 12–18 Mu-Mregion. J Atmos Sci 39:2923–2926

Kim ST, Cai W, Jin FF, Yu JY (2014) ENSO stability in coupled climate models and its association with mean state. Clim Dyn 42:3313–3321

Klein SA, Soden BJ, Lau NC (1999) Remote sea surface temperature variations during ENSO: evidence for a tropical atmospheric bridge. J Clim 12:917–932

Kobayashi S, Ota Y, Harada Y, Ebita A, Moriya M, Onoda H, Onogi K, Kamahori H, Kobayashi C, Endo H, Miyaoka K, Takahashi K (2015) The JRA-55 reanalysis: general specifications and basic characteristics. J Meteor Soc Jpn 93:5–48

Kociuba G, Power SB (2015) Inability of CMIP5 models to simulate recent strengthening of the walker circulation: Implications for projections. J Clim 28:20–35

Kosaka Y, Xie SP (2013) Recent global-warming hiatus tied to equatorial Pacific surface cooling. Nature 501:403–407

Kug JS, Ham YG, Lee JY, Jin FF (2012) Improved simulation of two types of El Niño in CMIP5 models. Environ Res Lett. doi:10.1088/1748-9326/7/3/034002

Li Y, Li JP, Zhang WJ, Zhao X, Xie F, Zheng F (2015) Ocean dynamical processes associated with the tropical Pacific cold tongue mode. J Geophys Res 120:6419–6435. doi:10.1002/2015JC010814

Li X, Xie SP, Gille ST, Yoo C (2016) Atlantic-induced pan-tropical climate change over the past three decades. Nat Clim Change 6:275–279

Luo JJ, Yamagata T (2001) Long-term El Niño-Southern Oscillation (ENSO)-like variation with special emphasis on the South Pacific. J Geophys Res 106(C10):22211–22227

Luo JJ, Masson S, Roeckner E, Madec G, Yamagata T (2005) Reducing climatology bias in an ocean–atmosphere CGCM with improved coupling physics. J Clim 18:2344–2360

Luo JJ, Sasaki W, Masumoto Y (2012) Indian Ocean warming modulates Pacific climate change. Proc Natl Acad Sci 109:18701–18706

Mantua NJ, Hare SR (2002) The Pacific decadal oscillation. J Oceanogr 58:35–44

Mantua NJ, Hare SR, Zhang Y, Wallace JM, Francis RC (1997) A Pacific interdecadal climate oscillation with impacts on salmon. Bull Amer Meteor Soc 78:1069–1079

Marotzke J, Forster PM (2015) Forcing, feedback and internal variability in global temperature trends. Nature 517:565–570

McGregor S, Timmermann A, Stuecker MF, England MH, Merrifield M, Jin FF, Chikamoto Y (2014) Recent Walker circulation strengthening and Pacific cooling amplified by Atlantic warming. Nat Clim Change 4:888–892

McPhaden MJ, Lee T, McClurg D (2011) El Niño and its relationship to changing background conditions in the tropical Pacific Ocean. Geophys Res Lett 38:L15709. doi:10.1029/2011GL048275

Meehl GA, Arblaster JM, Fasullo JT, Hu A, Trenberth KE (2011) Model-based evidence of deep-ocean heat uptake during surface-temperature hiatus periods. Nat Clim Change 1: 360–364

Meehl GA, Hu A, Arblaster M, Fasullo JT, Trenberth KE (2013) Externally forced and internally generated decadal climate variability associated with the Interdecadal Pacific Oscillation. J Clim 26:7298–7310

Meehl GA, Teng H, Arblaster JM (2014) Climate model simulations of the observed early-2000s hiatus of global warming. Nat Clim Change 4:898–902

Pan YH, Oort AH (1983) Global climate variations connected with sea surface temperature anomalies in the eastern equatorial Pacific Ocean for the 1958–1973 period. Mon Weather Rev 111:1244–1258

Philander SGH, Gu D, Lambert G, Li T, Halpern D, Lau NC, Pacanowski RC (1996) Why the ITCZ is mostly north of the Equator. J Clim 9:2958–2972

Power S, Casey T, Folland C, Colman A, Mehta V (1999) Inter-decadal modulation of the impact of ENSO on Australia. Clim Dyn 15:319–324

Rayner NA, Parker DE, Horton EB, Folland CK, Alexander LV, Rowell DP, Kent EC, Kaplan A (2003) Global analyses of sea surface temperature, sea ice, and night marine air temperature since the late nineteenth century. J Geophys Res 108(D14):4407. doi:10.1029/2002JD002670

Reynolds RW, Rayner NA, Smith TM, Stokes DC, Wang W (2002) An improved in situ and satellite SST analysis for climate. J Clim 15:1609–1625

Risbey JS, Lewandowsky S, Langlais C, Monselensan DP, O'Kane TJ, Oreskes N (2014) Well-estimated global surface warming in climate projections selected for ENSO phase. Nat Clim Change 4:835–840

Roberts CD, Palmer MD, McNeall D, Collins M (2015) Quantifying the likelihood of a continued hiatus in global warming. Nat Clim Change 5:337–342

Schmidt GA, Ruedy RA, Miller RL, Lacis AA (2010) Attribution of the present-day total greenhouse effect. J Geophys Res 115:D20106. doi:10.1029/2010JD014287

Schmidt GA, Shindell DT, Tsigaridis K (2014) Reconciling warming trends. Nat Geosci 7:158–160

Seager R, Murtugudde R (1997) Ocean dynamics, thermocline adjustment, and regulation of tropical SST. J Clim 10:521–534

Smith TM, Reynolds RW, Peterson TC, Lawrimore J (2008) Improvements to NOAA's historical merged land–ocean surface temperature analysis (1880–2006). J Clim 21:2283–2296

Smith DM, Booth BBB, Dunstone NJ, Eade R, Hermanson L, Jones GS, Scaife AA, Sheen KL, Thompson V (2016) Role of volcanic and anthropogenic aerosols in the recent global surface warming slowdown. Nat Clim Change 6:936–940

Solomon A, Newman M (2012) Reconciling disparate twentieth-century Indo-Pacific ocean temperature trends in the instrumental record. Nat Clim Change 2:691–699

Takahashi C, Watanabe M (2016) Pacific trade winds accelerated by aerosol forcing over the past two decades. Nat Clim Change 6:768–772

Taylor KE, Stouffer RJ, Meehl GA (2012) An overview of CMIP5 and the experiment design. Bull Amer Meteor Soc 93:485–498

Vecchi GA (2008) Examining the tropical Pacific's response to global warming. EOS 89(9):81–83

Watanabe M, Shiogama H, Tatebe H, Hayashi M, Ishii M, Kimoto M (2014) Contribution of natural decadal variability to global warming acceleration and hiatus. Nat Clim Change 4:893–897

Zhang Y, Wallace JM, Battisti DS (1997) ENSO-like interdecadal variability: 1900–93. J Clim 10:1004–1020

Zhang WJ, Li JP, Zhao X (2010) Sea surface temperature cooling mode in the Pacific cold tongue. J Geophys Res 115:C12042. doi:10.1029/2010JC006501